

Article

Characterization and In Vitro Studies of Low Reflective Magnetite (Fe₃O₄) Thin Film on Stainless Steel 420A Developed by Chemical Method

Reghuraj Aruvathottil Rajan ^{1,*}, Kaiprappady Kunchu Saju ¹ and Ritwik Aravindakshan ²

¹ Mechanical Engineering Division, School of Engineering, Cochin University of Science and Technology, Kalamassery, Cochin 682022, Kerala, India; kksaju@cusat.ac.in

² Mechanical Engineering Division, Toc H Institute of Science and Technology, Cochin 682314, Kerala, India; ritwik@tistcochin.edu.in

* Correspondence: reghuraj@alameen.edu.in

Abstract: Stainless steel has been the most demanded material for surgical utensil manufacture due to superior mechanical properties, sufficient wear, and corrosion resistance. Surgical grade 420A stainless steel is extensively used for producing sophisticated surgical instruments. Since these instruments are used under bright light conditions prevalent in operation theatres, the reflection from the material is significant which causes considerable strain to the eye of the surgeon. Surgical instruments with lower reflectance will be more efficient under these conditions. A low reflective thin-film coating has often been suggested to alleviate this inadmissible difficulty. This paper reports the development of an optimum parametric low reflective magnetite coating on the surface of SS 420A with a black color using chemical hot alkaline conversion coating technique and its bioactivity studies. Coating process parameters such as coating time, bath temperature, and chemical composition of bath are optimized using Taguchi optimization techniques. X-ray photoelectron spectroscopy (XPS) analysis was used to identify the composition of elements and the chemical condition of the developed coating. Surface morphological studies were accomplished with a scanning electron microscope (SEM). When coupled with an energy-dispersive X-ray analysis (EDAX), compositional information can also be collected simultaneously. In vitro cytotoxicity tests, corrosion behavior, the effect of sterilization temperature on adhesion property, and average percentage reflectance (R) of the developed coating have also been evaluated. These results suggest adopting the procedure for producing low reflective conversion coatings on minimally invasive surgical instruments produced from medical grade 420A stainless steel.



Citation: Aruvathottil Rajan, R.; Saju, K.K.; Aravindakshan, R. Characterization and In Vitro Studies of Low Reflective Magnetite (Fe₃O₄) Thin Film on Stainless Steel 420A Developed by Chemical Method. *Coatings* **2021**, *11*, 1145. <https://doi.org/10.3390/coatings11091145>

Academic Editor: Liqiang Wang

Received: 1 August 2021

Accepted: 14 September 2021

Published: 21 September 2021

Publisher's Note: MDPI stays neutral with regard to jurisdictional claims in published maps and institutional affiliations.



Copyright: © 2021 by the authors. Licensee MDPI, Basel, Switzerland. This article is an open access article distributed under the terms and conditions of the Creative Commons Attribution (CC BY) license (<https://creativecommons.org/licenses/by/4.0/>).

Keywords: magnetite; conversion coating; optimization; invitro cytotoxicity; corrosion

1. Introduction

Martensitic stainless steel of grade 410, 420A, 420B, and 420C has been widely used for the manufacturing of cutting and non-cutting surgical instruments [1,2]. In addition to biocompatibility, martensitic stainless steel has high strength, hardness, stiffness, rigidity, resilient, and non-corrosive nature [3]. Titanium (Ti) and its alloys are also used in various biomedical applications. Conventional as well as modern surface modification technologies have emerged in the recent decades. The mechanical, chemical, and biological properties are improved by adopting various surface modification methods. Conventional methods like sand blasting, alkali treatment, and plasma treatment have minor enhancements in the surface properties due to the intricate geometry of the work piece. To overcome these kinds of limitations, many modern surface modification methodologies such as laser surface modification, physical vapor deposition (PVD), and plasma spray-PVD show better performance in surface properties [4]. Key-hole or laparoscopic surgeries have been the focus of the emerging medical advancements. A detailed review of different

laparoscopic surgical staplers and mechanical components such as gears, links, pivots, and sliders used in performing their required functions is available. This aids in the identification of individual mechanisms used for certain tasks. It will make it easier to grasp the interrelationships between each sub-component that is required or will be used to complete difficult tasks [5]. Minimally invasive surgical instruments are generally made of 420A grade stainless steel. High intensity bright lights are used during minimally invasive or key-hole surgeries to improve the efficacy of surgeon by enhancing proper visualization of the operating field. But the reflection of incident light from the top layers of instruments hinders surgeon's visual field and leads to lack of precision in key-hole surgeries [6]. Low reflective top layers are key to reducing the disturbances caused due to reflection from bright surgical surfaces [7]. Conversion coating techniques are a widely used method for blackening ferrous materials. Hot aqueous alkaline process is a chemical conversion coating process. In such a process, the substrate surface is converted to black color due to chemical reaction between metal and molten salts, salt solution having an alkaline nature or with air at elevated temperatures [8]. The oxide layers developed on the substrate surface does not change the chemical state of the underlying surface.

In recent years various techniques have been adopted for blackening materials for different applications. Solar absorber made of AISI 316L has been deposited with a black coating using electrochemical deposition technique to reduce reflection [9]. Grey cast iron used for manufacturing electric stove was blackened by using a mixture of sodium hydroxide and sodium nitrate. The major component of the black oxide layer was magnetite and this oxide layer protects the hot plates of the electric stove [10]. The chemical conversion coating process has also been utilized to develop black formation on copper and its alloys. These coatings enhance bonding strength between copper and various polymers [11,12]. The anodizing method has been adopted to modify AZ31 Mg alloys to enhance corrosion resistance and biocompatibility, especially used for biomedical devices [13]. Electroless nickel coating technique has also been adopted to produce coating on the substrate surface to improve various properties of the base material [14]. A black film of titanium aluminum nitride and titanium carbon nitride has been produced on the stainless steel by physical vapor deposition which reduced the undesired light reflection, especially for minimally invasive surgical instruments [3,6]. Diamond-like carbon (DLC) coating has been developed on surgical instruments to enhance the intracorporeal instrument surface and durability of devices by using ionized evaporation method [15]. Despite the fact that many methods for coating metals with black oxide have been established, the scope of reducing reflection from surgical grade 420A stainless steel, which is extensively used for surgical instruments, has not been studied at length.

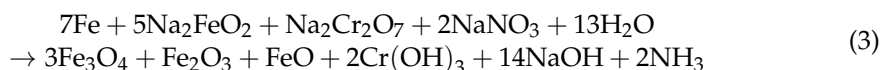
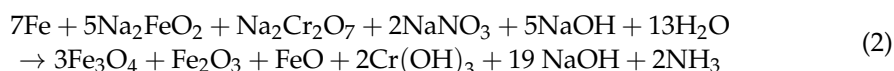
This paper reports the development of a black iron oxide (magnetite, Fe_3O_4) coating on the SS 420A surface using a hot aqueous alkaline treatment technique having a black color. The coating parameters such as coating duration, chemical composition of bath, temperature of salt solution, pickling effect, and pH value influence the anti-reflection characteristics of the coating developed [11,16–19]. Taguchi optimization technique was used to obtain optimal parameter low-reflective coating on the substrate surface. The XPS analysis, SEM analysis invitro toxicity, corrosion behavior, and sterilization effect of the developed coating were also studied extensively as a part of this research work.

2. Methodology

2.1. Sample Preparation and Coating Procedure

Surgical grade 420A stainless steel sample with the size of 25 mm × 25 mm × 3 mm has been produced from the ingot. The impurity from the surface was removed by blasting process. Glass beads with 60–80 screen size and 0.250–0.180 mm grain size were employed for an efficient blasting process. Further, it was degreased using an alkaline solution. The sample was pickled by using 20% dilute hydrochloric acid and cleaned in running water. For each experimental trial, laboratory-grade sodium hydroxide (NaOH), sodium nitrate (NaNO_3), and sodium dichromate ($\text{Na}_2\text{Cr}_2\text{O}_7$)—(Nice Chemicals Ltd., Kerala, India) were

dissolved in distilled water to prepare alkaline salt solution. The prepared alkaline mixture is poured into a stainless steel bath. The temperature of the bath can be controlled by using a regulator circuit together with a heating coil capable of heating 200 °C. Further, the samples were immersed inside the alkaline bath for the coating process. The Equations (1)–(3) describe the chemical reactions between stainless steel 420A and as prepared alkaline salt solution which causes the formation of magnetite. Further, the samples were cleaned in de-ionized water and allowed to dry in the air.



The ranges of coating parameters of the hot alkaline conversion treatment process were fixed by conducting numerous trials. The development of a homogeneous coating on the SS 420A surface is reliant on different coating variables, such as coating time, bath temperature, and chemical composition of salt solution. The alkaline salt solution is prepared by varying the weight percentage (wt.%) of sodium dichromate in the composition. Three different wt.% of sodium dichromate were considered. Wt.% of 250, 300, and 350 g/L were fixed after conducting the number of trial experiments. It was seen that no uniform black color coating was formed at less than 250 g/L and the coating changed into golden yellow color when we used more than 350 g/L. The coating time was adjusted between 50 and 60 min and the bath temperature was regulated between 115 and 125 °C. Experimental trials showed that lower bath temperature and duration in alkaline solution produced non-uniform black traces on the substrate surface. The duration and bath temperature above 60 min. and 125 °C lead to a change in color, which is undesirable. The wt.% of sodium hydroxide, sodium nitrate, and the pH value of the bath are maintained at constant values of 400 g/L, 320 g/L, and 8 respectively. The images of non-coated and coated stainless steel 420A substrate is as shown in Figure 1. The average percentage reflection (R) is a measurement of the amount of light reflected in the visible region from the substrate surface. A Varian Cary 5000 UV-VIS-NIR spectrophotometer (spectral range of 175–3300 nm, Agilent Technologies, Santa Clara, CA, USA) was used to measure the reflection of incident light (visible range) from the coated surface.

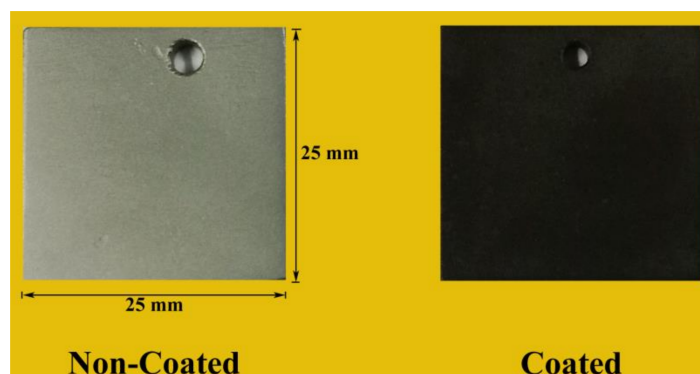


Figure 1. Non-coated and coated stainless steel 420A substrate.

2.2. Taguchi Design of Experiments

To determine the optimal parameter combination for minimizing the average percentage reflection (R), Taguchi orthogonal array (OA) was utilized. The coating time (D), bath temperature (T), and weight % of sodium dichromate (C) are selected as control elements and their levels are as shown in Table 1. The signal-to-noise (S/N) ratio was performed using Minitab-17 software. It is mainly categorized according to the required output char-

acteristics, that are lower-the-better, higher-the-better, or nominal-the-better [20]. Average percentage reflectance (R) should follow lower-the-better criteria, since lower R value is appreciable to obtain a low-reflective coating on SS 420A substrate surface. Higher-the-better condition is adopted to obtain the optimum combination of control factors from the main effect plot [21]. Since a high S/N ratio value indicates the optimum coating parameters in order to avoid the experimental noises as much as possible. Analysis of variance (ANOVA) and regression analysis were also conducted. Contour plots were used to investigate the relationship of output characteristics and two different control variables by analyzing discrete contours [22]. A conventional L9 OA for a 3 parameters 3 levels are as given in Table 2.

Table 1. Selected parameters and experimental levels.

Input Parameter	Symbol	Levels		
		A	B	C
Coating Time (min)	D	50	55	60
Bath temp (°C)	T	115 ± 2	120 ± 2	125 ± 2
Wt.% of sodium dichromate (g/L)	C	250	300	350

Table 2. The L9 OA, experimental results for avg. percentage reflectance.

Sample Code	OA			Avg. Percentage Reflectance	S/N Ratio
	D	T	C	R (%)	R (dB)
I	1	1	1	9.75	−19.7801
II	1	2	2	9.64	−19.6815
III	1	3	3	7.93	−17.9855
IV	2	1	2	9.01	−19.0945
V	2	2	3	8.21	−18.2869
VI	2	3	1	8.27	−18.3501
VII	3	1	3	7.9	−17.9525
VIII	3	2	1	9.04	−19.1234
IX	3	3	2	7.93	−17.9855

2.3. X-ray Photoelectron Spectroscopy (XPS)

XPS was used to identify the compositional and chemical states of the coating produced on the SS 420A substrate. Spectrum were plotted using a XPS, PHI 5000 Versa Probe II, (ULVAC-PHI Inc, Hagisono, Japan) having test parameters with beam spot of 200 μm, power of 15 KV monochromatic X-ray stimulation source Al-Kα (hv=1486.6 eV). Survey scans were recorded with an X-ray source power of 50 W and pass energy of 187.85 eV. High-resolution spectra of the major elements were recorded at 46.95 eV pass energy. The morphological studies and elemental composition of the coating were also analyzed using a scanning electron microscope (JEOL Model JSM-6390LV, JEOL, Tokyo, Japan) equipped with an energy dispersive X-ray analysis (EDAX, Oxford XMX N, Wiesbaden, Germany).

2.4. Cytotoxicity Assessment

Direct extract method according to ISO 10993-5 standard was used for invitro cytotoxicity assessment [23,24]. The L-929 cell line was used for the study. The coated and non-coated substrates were disinfected by autoclaving before conducting the assessment. The cultures were incubated in a minimum essential medium (MEM) supplemented with fetal bovine serum (FBS) for 24–26 h at 37 °C. For extract preparation, the disinfected specimens were submerged in the culture medium for 72 ± 2 h and kept at 50 ± 2 °C. Positive and negative controls were prepared by diluting phenol solution and incubating ultra-high molecular weight polyethylene (UHMWPE) for 72 ± 2 h at 50 ± 2 °C with culture medium. The prepared extract was adjusted to 100, 50, and 25 percentages respectively by mixing

the very similar cell culture. To determine the cytotoxic effects, various concentrations of test samples as well as positive and negative controls were seeded on the L-929 cell line and kept at 37 ± 1 °C for 24–26 h. The cellular reaction was investigated by analyzing the incubated cells cultured with positive, negative, and test controls using a microscope.

2.5. Corrosion Analysis

Quantitative assessment of corrosion was investigated using potentiodynamic polarization (PDP) tests according to ASTM standard G5-94 [25]. A standard three-electrode with 250 mL capacity cell was used for corrosion analysis. The electrochemical workstation was fitted with saturated calomel electrode (SCE) as the reference electrode, and platinum was employed as auxiliary electrode respectively. Coated, non-coated (control) SS 420A samples were used as working electrode during corrosion test. The electrolyte used for performing corrosion analysis was simulated body fluid (SBF) having a pH of 7.4 to create a natural tissue environment. The methodology adopted to create SBF was Kokubo method [26,27]. The SBF electrolyte was regulated at a temperature of 37 ± 1 °C.

A 1-cm² area of the working electrode was kept in contact with the prepared electrolyte. The specimens were allowed to remain in contact with the solution for duration of 3600 s until a constant open circuit potential (OCP) was achieved. The OCP was increased from an initial value of -1000 mV to 1000 mV. The sweep rate was set at 0.0005 mV/s. After conducting the potentiodynamic test on both the coated and non-coated SS 420A, Tafel extrapolation was conducted on polarization curves to calculate the corrosion current density (I_{corr}). The other corrosion parameters were measured to verify the corrosion resistance properties of non-coated and coated samples.

The ASTM B117 standard was followed for performing the salt spray test [28]. The reliability of the test is extremely influenced by the specimen type, evaluation criteria selected, and operating variables. The solution was formed by dissolving 5 ± 1 parts by mass of NaCl in 95 parts of water. The specific gravity and pH value was kept between 1.0268–1.0413 and 6.5–7.2 at 35 °C. During the testing, samples were exposed to a temperature of 35 ± 2 °C in the salt spray chamber for 24 h.

2.6. Repeated Sterilization and Morphology Studies

A repeated sterilization test was performed as per ISO 17665-1 standard for assessing the effect of sterilization temperature on the adhesion property of the black oxide coating [29]. In the conventional method, the temperature of the steam varies from 121–134 °C for a period of 15–21 min to ensure adequate sterilization. In rapid cycle, the samples were held at 134 °C for 3 min in an autoclave. To complete the sterilization process, samples were later allowed to cool. The entire sterilization procedure requires 45 min to one hour. Moreover, surface morphological studies of optimal parameter combination black oxide (Fe_3O_4)-coated SS 420A sample were accomplished with a scanning electron microscope (JEOL Model JSM-6390LV, JEOL, Tokyo, Japan).

3. Results and Discussion

3.1. Process Parameter Optimization

Table 2 shows the observed responses for different combinations of trials as well as the computed S/N ratios corresponding to avg. percentage reflectance (R). The obtained avg. S/N ratios for each level of input parameters are tabulated in Table 3. The ranks are assigned based on the statistical delta values. The parameter corresponding to the highest rank has a major influence on the coating process. From Figure 2, the highest mean S/N ratio for avg. percentage reflectance correspond to 60 min. coating time, 125 °C bath temperature, and 350 g/L wt.% of sodium dichromate. Therefore, the predicted optimal parameter combination for getting low avg. reflectance using Taguchi method were found as $D = 60$ min., $T = 125$ °C, and $C = 350$ g/L and it is represented as D3-T3-C3.

Table 3. Avg. S/N ratios for reflectance.

Level	D	T	C
1	−19.15	−18.94	−19.08
2	−18.58	−19.03	−18.92
3	−18.35	−18.11	−18.07
Delta	0.8	0.92	1.01
Rank	3	2	1

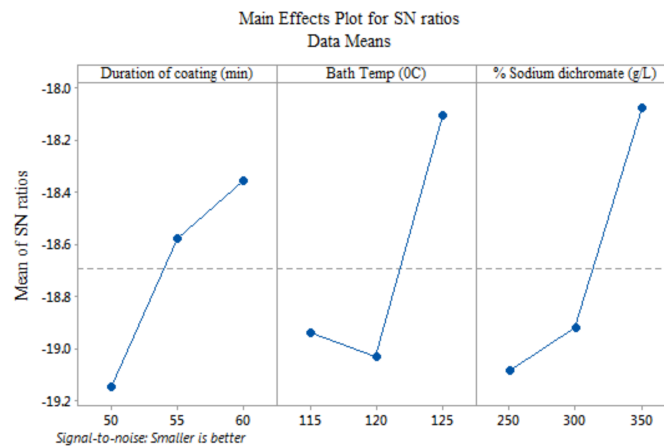


Figure 2. Mean effect plot for reflectance(R).

Table 4 shows the conformation test results for verifying Taguchi’s estimated avg. reflectance parameter combination. When comparing S/N ratios of estimated and optimum process parameters, it was found that they were almost identical. On comparing the S/N ratio value of the preliminary parameter combination, an improvement of 2.217 dB was noticed for the Taguchi estimated parameter combination. Additionally, the %R value decreased by 29.21% with respect to the preliminary parameter combination. Hence, the estimated ideal combination was adopted to produce an excellent low-reflective coating on stainless steel 420A with the least R value.

Table 4. Confirmation test for Taguchi predicted optimum parameter combination.

Output Characteristics	Preliminary Parameter Combination	Optimal Combination of Parameter	
		Predicted Values	Experimental Values
Level	D1-T1-C1	D3-T3-C3	D3-T3-C3
Avg. reflectance (%)	9.75	D3-T3-C3	7.546
S/N ratio (dB)	−19.7801	−17.1491	−17.5631
S/N ratio enhancements (dB)	2.217	-	-
Percentage decrement in R	29.21%	-	-

Analysis of variance (ANOVA) results were obtained corresponding to the output characteristics and summarized in Table 5. The *p* values corresponding to input parameters clearly depict the considerable influence of parameters during magnetite formation on SS 420A. The contributions of each parameter in terms of percentage were calculated and wt.% of sodium dichromate has remarkable influence in the formation of magnetite.

Equation (4) shows the mathematical model was formulated between output characteristics and input variables using regression analysis. The corresponding R-sq value is 85.41%, which denotes the effectiveness of the developed linear regression equation in predicting R within the given input range. The confirmation tests were also conducted to verify the validity of the developed mathematical model. Taguchi predicated optimum combination was considered as input values and the obtained results are summarized

in Table 6. From the table, it is observed that, the R value predicted by the formulated mathematical model is nearer to the experimental results, which is desirable.

$$\text{Avg. percentage reflectance (R)} = 26.26 - 0.0817 \times (\text{D}) - 0.0843 \times (\text{T}) - 0.01007 \times (\text{C}) \quad (4)$$

Table 5. ANOVA results for average reflectance value (R).

Parameters	DF	SS	MS	F	P	% Contribution
Coating time (D)	2	1.08179	0.54088	224.33	0.004	24.55
Bath temp (T)	2	1.56349	0.78174	324.23	0.003	35.49
wt.% of Na ₂ Cr ₂ O ₇ (C)	2	1.75582	0.87991	364.11	0.003	39.85
Error	2	0.00482	0.00241	-	-	-
Total	8	4.40589	-	-	-	-

Table 6. Validation of developed mathematical model.

Coating Characteristics	Optimal Parameter Combination	Predicted Value	Experimental Value
Reflectance (R)	D3-T3-C3 (60 min, 125 °C, 350 g/L)	7.296%	7.546%

Figure 3A–C shows the contour plots that illustrate the desirable average percentage reflectance and corresponding control factors. It is seen that higher bath temperature, longer coating duration, and larger wt.% of sodium dichromate lead to generate coating with low reflectance.

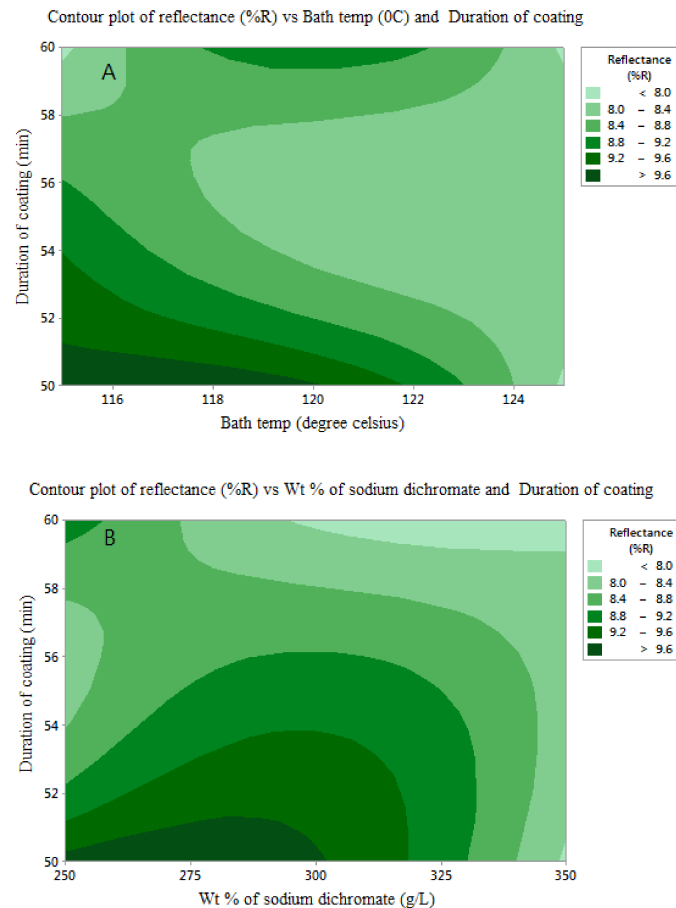


Figure 3. Cont.

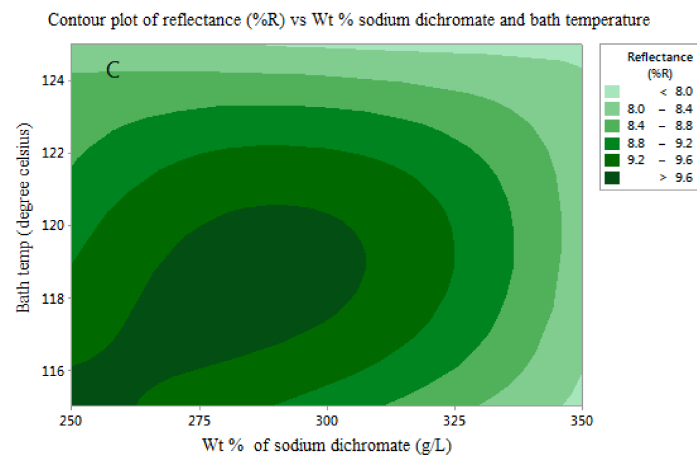


Figure 3. (A) Effect of bath temperature and duration of coating on reflectance. (B) Effect of wt.% of sodium dichromate and duration of coating on reflectance. (C) Effect of wt.% of sodium dichromate and bath temperature on reflectance.

3.2. XPS Analysis of Coating

The surface survey according to XPS indicated the presence of C 1s (85.3%), O 1s (14.1%), Fe 2p_{3/2} (0.4%), and Cr 2p_{3/2} (0.17%) as in Figure 4. Figure 5A,B represents the high resolution spectrum of C 1s and O 1s. The Fe 2p_{3/2} spectrum was fitted with major and minor peaks of Fe³⁺ and Fe²⁺ corresponding to the binding energy of 712.4 eV and 709.9 eV as shown in Figure 5C and it is well in accordance with the values of magnetite found. The details about FeO and γ -Fe₂O₃ can be provided easily by separating the corresponding satellite structure [30]. Therefore, the developed black oxide coating is magnetite (Fe₃O₄) [31,32]. The high-resolution spectrum of Cr 2p_{3/2} displays metallic species of Cr and formation of Cr₂O₃ corresponding to 573.6 eV and 576.1 eV respectively as in Figure 5D. The multiplet splitting at Cr 2p_{3/2} peak is only because of the presence of chromic oxide (Cr³⁺) since only trivalent chromium out of the possible oxides of Cr shows pronounced multiplet splitting [33]. To ensure the presence of chromium, the elemental composition of the coating is also analyzed by SEM-EDAX. From Figure 6, the presence of chromium is ensured in the developed coating.

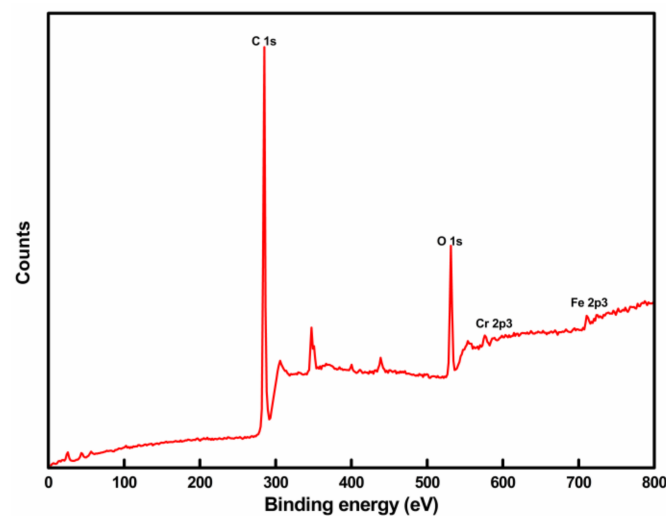


Figure 4. The XPS survey spectra recorded from a thin film magnetite on SS 420A.

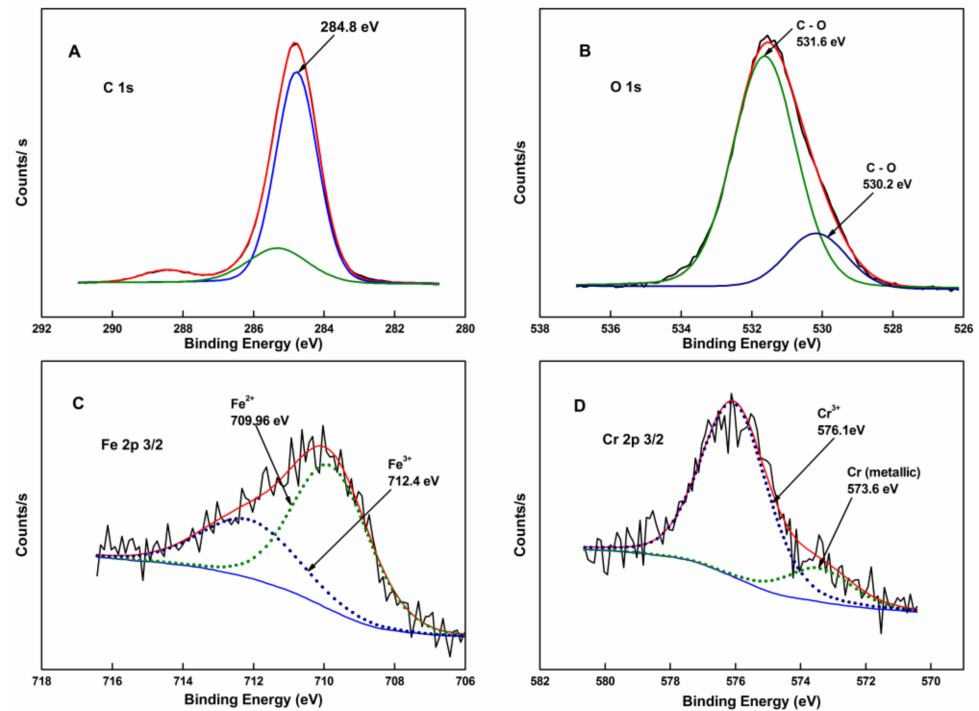


Figure 5. The XPS high-resolution spectrum from the fractured surface of coated sample (A) C 1s, (B) O 1s, (C) Fe 2p_{3/2}, (D) Cr 2p_{3/2}.

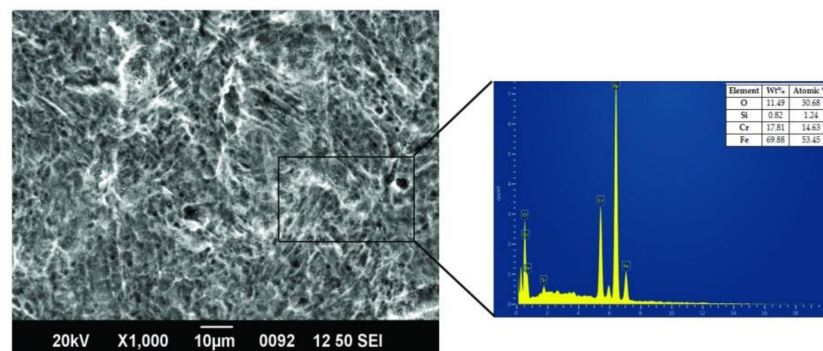


Figure 6. Microstructure and EDAX spectra of Fe₃O₄-coated SS 420A.

3.3. In Vitro Cytotoxicity Study

Cellular response of L-929 cell line cultured with extracts of different samples was graded and evaluated. The cytotoxicity was evaluated by comparing the cell response grade of test samples with negative and positive controls. Negative and positive controls gave grades 0 and 4 as expected. The three diluted extracts, 100%, 50%, and 25% of non-coated (control) and coated SS 420A samples have given a grade of 2, which is acceptable by ISO 10993-5 [23,24]. Figure 7A–F are the microscopic images of the L-929 cell line exposed for a duration of 24 h with 100%, 50% and 25% proportions of extracts of non-coated and coated SS 420A. From the figure, it has been shown that up to 50% of cells are round, devoid of cytoplasmic fine particles, showing no cellular lysis, with vacant spaces between cells. These findings suggest that the developed low reflective chemically formed magnetite on stainless steel 420A is non-toxic.

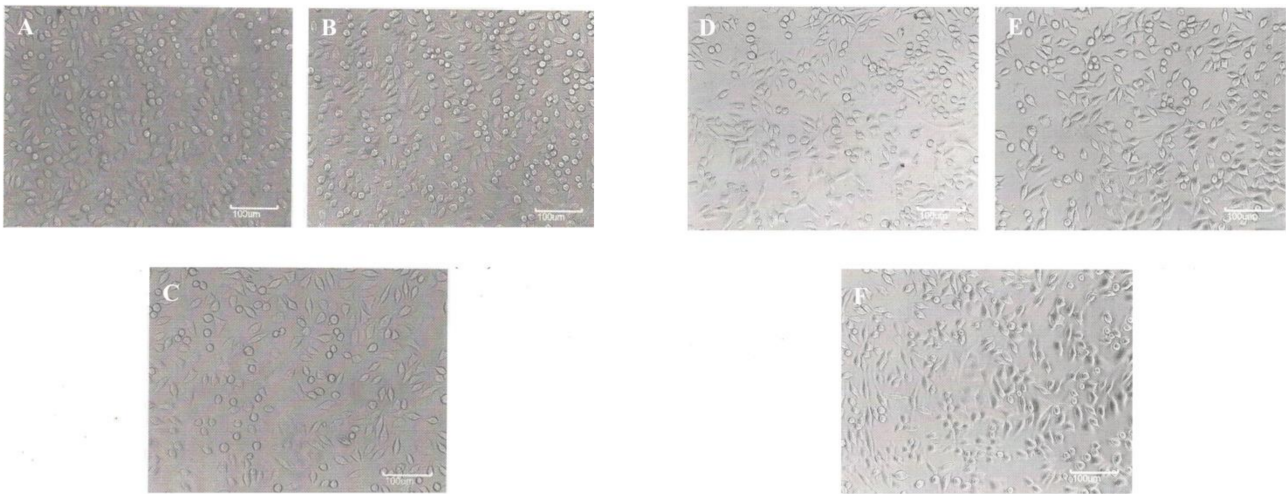


Figure 7. Microscopic image of L-929 cells exposed to different proportions (100%, 50% and 25%) of extract media of (A–C) non-coated SS 420A (D–F) coated SS 420.

3.4. Potentiodynamic Polarization and Salt Spray Studies

The corrosion behavior of control and coated SS 420A was evaluated using an electrochemical workstation together with simulated body fluid (SBF) environment and repeated at least three times. The polarization curves for different samples are given in Figure 8. The measured electrochemical parameters from PDP curves are tabulated in Table 7. From the table, it was noticed that corrosion current density (I_{corr}) having a strict linear relationship with corrosion rate (CR). Thus, the lower the I_{corr} value the greater the resistance to corrosion [34]. Hence the magnetite over-layered SS 420A sample has slight improvement in resistance to accelerated corrosion. Moreover, the higher E_{corr} value of magnetite layered SS 420A, indicates chemical inertness and the lowest corrosion tendency. The measured R_p value also indicates that the coated substrate shows slight improvement against applied accelerated corrosion compared to the non-coated SS 420A. The corrosion resistance of coated samples was also verified by the salt spray test. Samples were visually inspected and no rust was formed after 24 h test and it shows the developed coating can withstand corrosion.

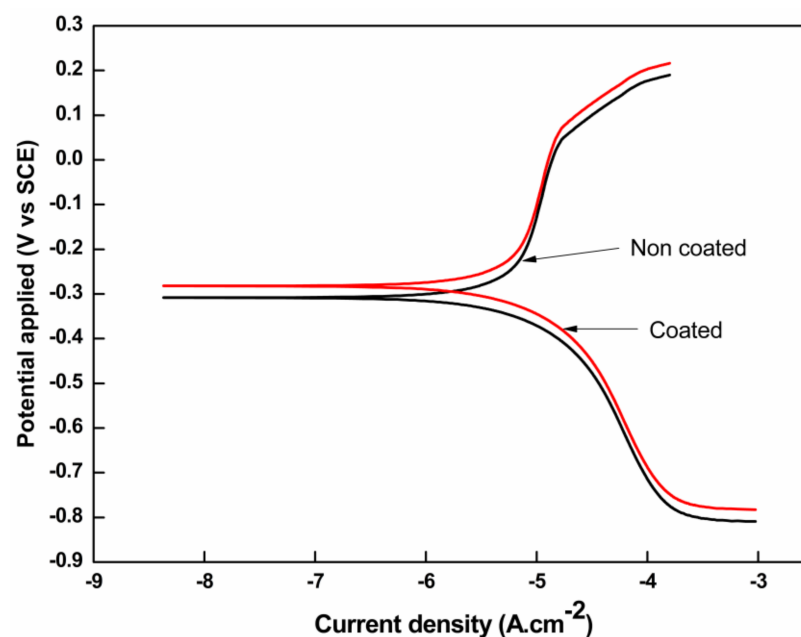


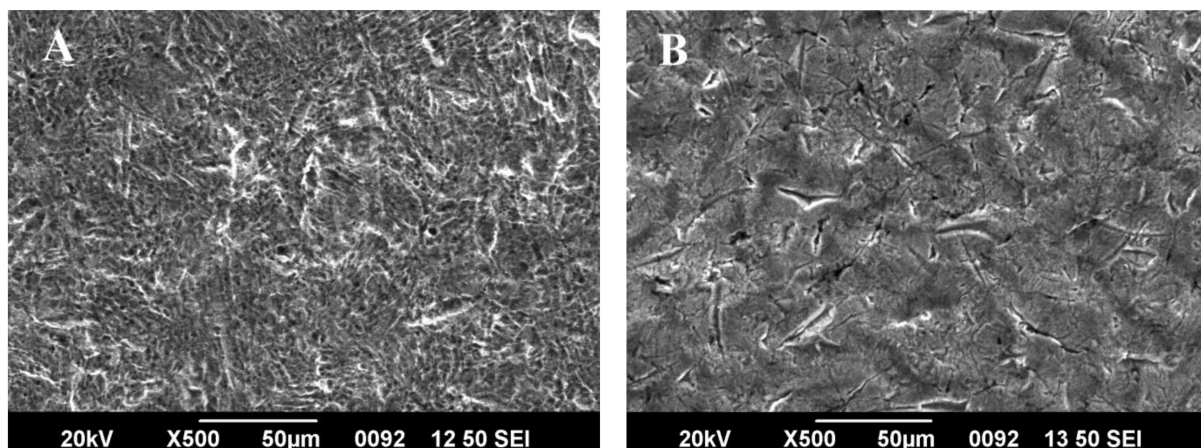
Figure 8. Potentiodynamic polarization curves of non-coated (control) and coated SS 420A.

Table 7. Polarization parameters of coated and non-coated SS 420A in SBF.

Sample	Corrosion Parameters					
	E_{corr} (mv)	I_{corr} (mA/cm ²)	β_a (mV·decade ⁻¹)	β_c (mV·decade ⁻¹)	R_p (Ω Cm ²)	Corrosion Rate (mm/y)
SS 420A Coated Sample	−283.57	0.0239	−910.88	392.74	8855.7	0.310
SS 420A Non coated (Control Sample)	−308.51	0.0351	−863.36	379.16	8029.1	0.413

3.5. Effect of Repeated Sterilization on Coating

The SEM images (20 kV and 1000× magnification) of coated samples before and after conducting 100 cycles of repeated sterilization as per ISO standards are shown in Figure 9. No damages like discoloration peel off were observed after the repeated autoclaving process. From Figure 9B, minor stress relief cracks were observed. This is due to sudden cooling of the coating and the substrate from treatment temperature to room temperature [35]. If the developed coating detaches due to the sterilization temperature from the instrument during the surgery, it can lead to serious damages to surrounding tissues. The average percentage reflectance (R) value was measured to analyze the effect of repeated sterilization on coatings. The average percentage reflectance graph of coated SS420A before and after steam sterilization is given in Figure 10A,B. The measured average percentage reflectance value of coated substrate before steam sterilization is 7.546%. From Figure 10B, the coating exhibits excellent antireflective property with a minimum R value in the visible region of 8.32% after undergoing 100 cycles of repeated sterilization on uniform black magnetite forming SS 420A. There is smaller variation in the R value of coated sample before and after repeated sterilization procedure. Even though the reflection of light comparatively is much lesser than not coated SS 420A. This indicates, repeated sterilization does not adversely affect the antireflective property of the developed coating.

**Figure 9.** SEM images of coated SS 420A (A) before sterilization (B) after 100 cycles of sterilization.

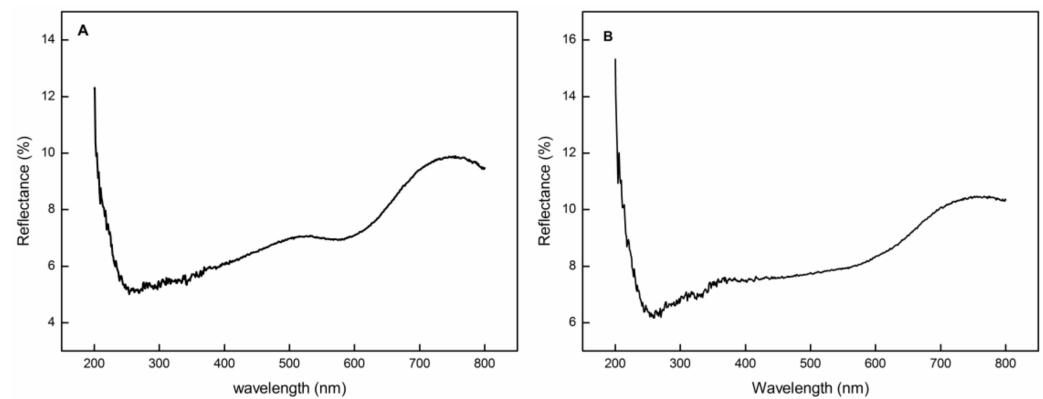


Figure 10. The average percentage of reflectance in the visible region (A) before steam sterilization (B) after 100 cycles of steam sterilization.

4. Conclusions

A low reflective black iron oxide (magnetite) coating was produced on stainless steel 420A using chemical hot aqueous alkaline conversion coating technique. The coating parameter values of alkaline conversion coating process were optimized using the Taguchi optimization technique. The optimum coating parameter combination for minimum average percentage reflection (R) value is obtained as D3-T3-C3 (D = 60 min., T = 125 °C and C = 350 g/L). The R value of uniform black coated SS 420A is reduced to 7.546% from a value of 56.14% of non-coated samples. It is seen that the chemical composition of bath and bath temperature has greatest impact in magnetite formation on SS 420A. This coating reduces the undesired difficulties of surgeons due to scattering and reflection of incident light in the visible spectrum from the exteriors of surgical equipment manufactured by SS 420A. The developed coating was characterized using XPS analysis and the formation of magnetite (Fe_3O_4) was identified. An invitro cytotoxicity test was performed using the L-929 cell line and confirmed the non-toxic behavior of the developed coating. Corrosion studies showed that magnetite layered SS 420A has better corrosion resistance properties than the non-coated substrate. A repeated sterilization test was conducted to measure the ability of the developed coating to withstand the sterilization process. The average percentage reflectance (R) value slightly increased to 8.32% after 100 cycles of autoclaving, which is desirable. These results suggest that the developed coating may be used for producing a biocompatible low-reflective black coating for surgical equipment composed of medical grade 420A stainless steel.

Author Contributions: R.A.R., contributed to the experimental and analytical work of the research; K.K.S., contributed to the validation and evaluation of the findings reported in the paper; R.A., contributed to evaluation of the findings. All authors have read and agreed to the published version of manuscript.

Funding: We did not receive any specific grant from funding agencies in the public, commercial, or not-for-profit sectors.

Institutional Review Board Statement: Not applicable.

Informed Consent Statement: Not applicable.

Data Availability and Statement: The authors declare that data supporting the findings of this study are available within the article.

Acknowledgments: We would like to thank DST-SAIF, Cochin, NIIST Trivandrum, ICAR-CIFT, Cochin and Jayon Implants, Palakkad, for providing all necessary support towards this research work.

Conflicts of Interest: The authors declare that they have no conflict of interests.

Nomenclature

SS	Stainless steel
XPS	X-ray photoelectron spectroscopy
R	Average percentage reflection
AISI	American iron and steel institute
DLC	Diamond-Like Carbon
CVD	Chemical vapor deposition
PVD	Physical vapor deposition
wt.%	Weight percentage
D	Duration of coating
T	Bath temperature
C	wt% of sodium dichromate
S/N	Signal-to-noise
OA	Orthogonal Array
DF	Degrees of freedom
SS	Sum of squares
MS	Mean square
F	Fisher's ratio
P	Probability value
MEM	Minimum essential medium
FBS	Fetal bovine serum
UHMWPE	Ultra-high molecular weight polyethylene
SCE	Saturated calomel electrode
PDP	Potentiodynamic polarization
SBF	Simulated body fluid
OCP	Open circuit potential
I_{corr}	Corrosion current
E_{corr}	Corrosion potential
R_p	Polarization resistance
β_a	Anodic Tafel slope
β_c	Cathodic Tafel slope
CR	Corrosion rate

References

1. Festas, A.; Ramos, A.; Davim, J.P. Medical devices biomaterials—A review. *Proc. Inst. Mech. Eng. Part L J. Mater. Des. Appl.* **2019**, *234*, 218–228. [[CrossRef](#)]
2. Chauhan, L.R.; Singh, M.; Bajpai, J.K.; Misra, K.; Agarwal, A. Development of chemical conversion coating for blackening of a grade of stainless steel useful for fabrication of optical devices. *J. Surf. Sci. Technol.* **2017**, *32*, 99. [[CrossRef](#)]
3. Ali, S.; Rani, A.M.A.; Baig, Z.; Ahmed, S.W.; Hussain, G.; Subramaniam, K.; Hastuty, S.; Rao, T.V. Biocompatibility and corrosion resistance of metallic biomaterials. *Corros. Rev.* **2020**, *38*, 381–402. [[CrossRef](#)]
4. Zhang, L.-C.; Chen, L.-Y.; Wang, L. Surface modification of titanium and titanium alloys: Technologies, developments, and future interests. *Adv. Eng. Mater.* **2020**, *1*–16. [[CrossRef](#)]
5. Lim, J.J.; Erdman, A.G. A review of mechanism used in laparoscopic surgical instruments. *Mech. Mach. Theory* **2003**, *38*, 1133–1147. [[CrossRef](#)]
6. Hollstein, F.; Louda, P. Bio-compatible low reflective coatings for surgical tools using reactive d.c.-magnetron sputtering and arc evaporation—a comparison regarding steam sterilization resistance and nickel diffusion. *Surf. Coat. Technol.* **1999**, *120–121*, 672–681. [[CrossRef](#)]
7. Reghuraj, A.; Saju, K. Black oxide conversion coating on metals: A review of coating techniques and adaptation for SAE 420A surgical grade stainless steel. *Mater. Today Proc.* **2017**, *4*, 9534–9541. [[CrossRef](#)]
8. Ooi, S.W.; Yan, P.; Vegter, R.H. Black oxide coating and its effectiveness on prevention of hydrogen uptake. *Mater. Sci. Technol.* **2018**, *35*, 12–25. [[CrossRef](#)]
9. Lira-Cantú, M.; Sabio, A.M.; Brustenga, A.; Gomez-Romero, P. Electrochemical deposition of black nickel solar absorber coatings on stainless steel AISI316L for thermal solar cells. *Sol. Energy Mater. Sol. Cells* **2005**, *87*, 685–694. [[CrossRef](#)]
10. Nagode, A.; Klančnik, G.; Schwarczova, H.; Kosec, B.; Gojić, M.; Kosec, L. Analyses of defects on the surface of hot plates for an electric stove. *Eng. Fail. Anal.* **2012**, *23*, 82–89. [[CrossRef](#)]
11. Lebbai, M.; Kim, J.-K.; Szeto, W.K.; Yuen, M.M.F.; Tong, P. Optimization of black oxide coating thickness as an adhesion promoter for copper substrate in plastic integrated-circuit packages. *J. Electron. Mater.* **2003**, *32*, 558–563. [[CrossRef](#)]

12. Kim, J.-K.; Woo, R.S.; Hung, P.Y.; Lebbai, M. Adhesion performance of black oxide coated copper substrates: Effects of moisture sensitivity test. *Surf. Coat. Technol.* **2006**, *201*, 320–328. [[CrossRef](#)]
13. Zaffora, A.; Di Franco, F.; Virtù, D.; Pavia, F.C.; Ghersi, G.; Virtanen, S.; Santamaria, M. Tuning of the Mg alloy AZ31 anodizing process for biodegradable implants. *ACS Appl. Mater. Interfaces* **2021**, *13*, 12866–12876. [[CrossRef](#)]
14. Sarkar, S.; Mukherjee, A.; Baranwal, R.K.; De, J.; Biswas, C.; Majumdar, G. Prediction and parametric optimization of surface roughness of electroless Ni-Co-P coating using Box-Behnken design. *J. Mech. Behav. Mater.* **2019**, *28*, 153–161. [[CrossRef](#)]
15. Kaneko, M.; Hiratsuka, M.; Alanazi, A.; Nakamori, H.; Namiki, K.; Hirakuri, K. Surface reformation of medical devices with DLC coating. *Materials* **2021**, *14*, 376. [[CrossRef](#)]
16. Sharma, A.; Rani, R.U.; Mayanna, S. Thermal studies on electrodeposited black oxide coating on magnesium alloys. *Thermochim. Acta* **2001**, *376*, 67–75. [[CrossRef](#)]
17. Tepe, B.; Gunay, B. Evaluation of pre-treatment processes for HRS (hot rolled steel) in powder coating. *Prog. Org. Coat.* **2008**, *62*, 134–144. [[CrossRef](#)]
18. Li, G.; Niu, L.; Lian, J.; Jiang, Z. A black phosphate coating for C1008 steel. *Surf. Coat. Technol.* **2004**, *176*, 215–221. [[CrossRef](#)]
19. Zhao, M.; Wu, S.; Luo, J.; Fukuda, Y.; Nakae, H. A chromium-free conversion coating of magnesium alloy by a phosphate–permanganate solution. *Surf. Coat. Technol.* **2006**, *200*, 5407–5412. [[CrossRef](#)]
20. Mohsin, I.; He, K.; Li, Z.; Zhang, F.; Du, R. Optimization of the polishing efficiency and torque by using taguchi method and ANOVA in robotic polishing. *Appl. Sci.* **2020**, *10*, 824. [[CrossRef](#)]
21. Zalnezhad, E.; Sarhan, A.A.D.; Hamdi, M. Optimizing the PVD TiN thin film coating’s parameters on aerospace AL7075-T6 alloy for higher coating hardness and adhesion with better tribological properties of the coating surface. *Int. J. Adv. Manuf. Technol.* **2012**, *64*, 281–290. [[CrossRef](#)]
22. Kumar, S.; Singh, R.; Jaiswal, R.; Kumar, A. Optimization of process parameters of electron beam welded Fe49Co2V alloys. *Int. J. Eng. Trans. B Appl.* **2020**, *33*, 870–876. [[CrossRef](#)]
23. Liu, X.; Rodeheaver, D.P.; White, J.C.; Wright, A.M.; Walker, L.M.; Zhang, F.; Shannon, S. A comparison of in vitro cytotoxicity assays in medical device regulatory studies. *Regul. Toxicol. Pharmacol.* **2018**, *97*, 24–32. [[CrossRef](#)]
24. Vidal, M.N.P.; Granjeiro, J.M. Cytotoxicity tests for evaluating medical devices: An alert for the development of biotechnology health products. *J. Biomed. Sci. Eng.* **2017**, *10*, 431–443. [[CrossRef](#)]
25. Farzam, M.; Baghery, P.; Dezfally, H.R.M. Corrosion study of steel API 5A, 5L and AISI 1080, 1020 in drill-mud environment of Iranian hydrocarbon fields. *Int. Sch. Res. Not.* **2011**, *2011*, 681535. [[CrossRef](#)]
26. Zaludin, M.A.F.; Jamal, Z.A.Z.; Derman, M.N.; Kasmuin, M.Z. Fabrication of calcium phosphate coating on pure magnesium substrate via simple chemical conversion coating: Surface properties and corrosion performance evaluations. *J. Mater. Res. Technol.* **2019**, *8*, 981–987. [[CrossRef](#)]
27. Kokubo, T.; Takadama, H. How useful is SBF in predicting in vivo bone bioactivity? *Biomaterials* **2006**, *27*, 2907–2915. [[CrossRef](#)] [[PubMed](#)]
28. Mitchell, J.; Crow, N.; Nieto, A. Effect of surface roughness on pitting corrosion of AZ31 Mg Alloy. *Metals* **2020**, *10*, 651. [[CrossRef](#)]
29. Vannozzi, L.; Catalano, E.; Telkhozhayeva, M.; Teblum, E.; Yarmolenko, A.; Avraham, E.S.; Konar, R.; Nessim, G.D.; Ricotti, L. Graphene oxide and reduced graphene oxide nanoflakes coated with glycol chitosan, propylene glycol alginate, and poly-dopamine: Characterization and cytotoxicity in human chondrocytes. *Nanomaterials* **2021**, *11*, 2105. [[CrossRef](#)] [[PubMed](#)]
30. Ramazanov, S.; Sobola, D.; Orudzhev, F.; Knápek, A.; Polčák, J.; Potoček, M.; Kaspar, P.; Dallaev, R. Surface modification and enhancement of ferromagnetism in BiFeO₃ nanofilms deposited on HOPG. *Nanomaterials* **2020**, *10*, 1990. [[CrossRef](#)] [[PubMed](#)]
31. Yamashita, T.; Hayes, P. Analysis of XPS spectra of Fe²⁺ and Fe³⁺ ions in oxide materials. *Appl. Surf. Sci.* **2008**, *254*, 2441–2449. [[CrossRef](#)]
32. Grosvenor, A.; Kobe, B.A.; Biesinger, M.C.; McIntyre, N.S. Investigation of multiplet splitting of Fe 2p XPS spectra and bonding in iron compounds. *Surf. Interface Anal.* **2004**, *36*, 1564–1574. [[CrossRef](#)]
33. Liu, R.; Conradie, J.; Erasmus, E. Comparison of X-ray photoelectron spectroscopy multiplet splitting of Cr 2p peaks from chromium tris(β-diketonates) with chemical effects. *J. Electron Spectrosc. Relat. Phenom.* **2016**, *206*, 46–51. [[CrossRef](#)]
34. Faghani, G.; Rabiee, S.M.; Nourouzi, S.; Elmkhah, H. Corrosion behavior of TiN/CrN nanoscale multi-layered coating in Ringer’s solution. *Int. J. Eng.* **2020**, *33*, 329–336. [[CrossRef](#)]
35. Hanoz, D.; Settimi, A.G.; Dabalà, M. Characterization of black coating on Fe360 steel obtained with immersion in aqueous solutions. *Surf. Interfaces* **2021**, *26*, 101317. [[CrossRef](#)]